Bio-Inspired Adaptive Control for Active Knee Exoprosthetics

Anna Pagel, Raffaele Ranzani, Robert Riener, and Heike Vallery

***Abstract*— On the quest to bring function of prosthetic legs closer to their biological counterparts, the intuitive interplay of their control with the user's impedance modulation is key. We present two control features to enable more physiological and more user-adaptive control of prosthetic legs: a neuromusculoskeletal impedance model (*NeurImp*) including a reflexive component, and a human model reference adaptive controller (*HuMRAC*), which can be combined with the former. In stance-phase simulations, the *NeurImp* allowed to control a prosthetic leg with physiological knee joint angle and moment. When perturbations were applied, the *HuMRAC* reduced the resulting root mean square error (RMSE) between simulated and physiological reference angle by 96%. In a pilot experiment with two unimpaired and one amputee subject, gait with the *NeurImp* deviated more from a physiological reference than with a conventional visco-elastic impedance controller. Subjects, however, preferred the *NeurImp*. When adding the *HuMRAC* to either of the two impedance controllers, the RMSE between the actual and the physiological reference angle was reduced by up to 54%. Subjects confirmed this finding and reported an easier stance-to-swing transition. Simulation and pilot experiment suggest that a reflex-based impedance controller combined with an adaptive controller may improve user-cooperative behavior of active knee exoprostheses.**

***Index Terms*— Active knee exoprosthetics, adaptive control, joint impedance modulation, reflex-based neuromusculoskeletal model, user-cooperative control.**

I. Introduction

OVER the last decades, research groups and companies worldwide have made great advances developing hardware and controllers for active knee exoprostheses. While dimensions, weight and actuation principles are already similar to the biological archetype [1], it still remains challenging to design controllers that replicate the human locomotor control, i.e. the central nervous system. Although it may not be necessary to duplicate the human locomotor system [2], a bio-inspired control should allow for different functionalities like level-ground walking and stair climbing, as well as for physiological gait patterns. This includes the correct kinematics as well as physiological impedance modulation and adaptation. Furthermore, the control of the prosthesis should at any time be user-cooperative, intuitive and safe.

Today, the most widely-used control paradigm for active knee prosthetics is a hierarchical controller which combines a finite-state machine (FSM) with variable impedance control [3]–[7]. The variable impedance generally includes two components: a virtual rotational spring and a virtual rotational damper. The stiffness and setpoint of the spring and the damping coefficient vary depending on the gait phase, which is detected using sensory information from the prosthesis. This virtual impedance mimics the behavior of the human knee during walking well if the correct stiffness and damping parameters are chosen [8].

However, knowledge about physiological impedance values and impedance modulation is limited. Therefore, all parameters are usually manually tuned, which can be a time-consuming and tedious procedure, or automatically determined to replicate a physiological joint trajectory [9]. Alternatively, we proposed a model-based approach to estimate joint stiffness [10], and we recently used the obtained values for visco-elastic impedance control of an actuated prosthesis [11].

Another limitation of the above control schemes is the missing ability to adapt to changes in the environment, which is a fundamental characteristic of human motor control. Humans are able to subconsciously adapt to unexpected interactions with the environment through reflexive mechanisms [12], [13]. An alternative approach to classical impedance models that tries to realize this adaptivity is based on a muscle-reflex model [14]–[16]. The model includes several muscle-tendon units which are comprised of a Hill-type muscle with a positive force feedback reflex scheme and two parallel and one series elasticity. Simulations revealed that this model can replicate gait dynamics and kinematics and tolerates ground disturbances and different slopes. In a controller for an actuated ankle-foot prosthesis, a combination of this neuromuscular model that acts as plantarflexor and a virtual rotary spring-damper that acts as dorsiflexor was implemented [17]. Parameters of the

Manuscript received December 11, 2016; revised July 28, 2017; accepted August 20, 2017. Date of publication August 25, 2017; date of current version November 29, 2017. This work was supported in part by the Swiss National Science Foundation through the National Centre of Competence in Research Robotics, in part by the Gottfried und Julia Bangerter-Rhyner Stiftung, in part by an ETH Research Grant, and in part by the Marie-Curie Career Integration under Grant PCIG13-GA-2013-618899. *(Anna Pagel and Raffaele Ranzani are co-first authors.) (Corresponding author: Anna Pagel.)*

A. Pagel and R. Riener are with the Sensory-Motor Systems Laboratory, Department of Health Sciences and Technology, ETH Zürich, Zürich, Switzerland, and also with the Medical Faculty, University of Zürich, Zürich, Switzerland (e-mail: pagel.anna@alumni.ethz.ch).

R. Ranzani is with the Rehabilitation Engineering Laboratory, Department of Health Sciences and Technology, ETH Zürich, Zürich, Switzerland.

H. Vallery is with the Delft Robotics Laboratory, Delft University of Technology, Delft, The Netherlands.

Digital Object Identifier 10.1109/TNSRE.2017.2744987

muscle-tendon complex and the dorsiflexor were optimized with respect to the joint moment profile of physiological gait.

In this manuscript, a bio-inspired impedance controller is proposed that tries to achieve both

1) physiological modulation of joint dynamics, i.e. joint angle, angular velocity and moment, during level-ground walking and
2) adaptation of these joint dynamics to account for unmodeled effects such as differences in physiology as well as differences between sound and prosthetic leg.

To achieve the first goal, a neuromusculoskeletal impedance model (*NeurImp*) is implemented. The *NeurImp* is inspired by intrinsic and reflexive pathways in the human motor control system.

To achieve the second goal, a Human Model Reference Adaptive Controller (*HuMRAC*) is used to adapt the knee joint angle and moment while allowing for increased interaction of the user with the prosthesis. The *HuMRAC* is inspired by optimality principles in human motor control and is based on models of human physiology [18].

First, the two control features were tested in a simulation environment to assess their properties and performance. Second, the two control features were implemented on the ANGELAA active knee exoprosthesis that has been developed in our group [11]. A pilot experiment with two unimpaired and one amputee subject were conducted where the *NeurImp* and a conventional visco-elastic impedance model were tested alone and in combination with the *HuMRAC*.

II. Development of a Bio-Inspired Controller

Figure 1 summarizes the control idea presented in this manuscript. The selected impedance model translates kinematics (joint angle θ_K and angular velocity $\dot{\theta}_K$) and kinetics (joint moment τ_K) of the prosthetic joint to a desired joint torque u_m. The adaptive controller can optionally be switched on to provide the adaptive knee joint moment τ_a. Following [19], the reference trajectory θ_{ref} for the adaptive controller is calculated from residual body motion $\boldsymbol{x}_{res}$, here the movement of the contralateral thigh and shank. A FSM provides the control parameters to the impedance model. A PI-controller calculates the required motor torque τ_{mot}.

A. Neuromusculoskeletal Impedance Model

Most variable-impedance controllers for active prostheses incorporate a virtual spring with time-dependent stiffness $K(t)$ and a virtual damper with damping $B(t)$ that form the virtual impedance and reflect the visco-elastic muscle behavior [20]. The two parameters and the piecewise constant setpoint angle $\theta_{set}(t)$ as function of time t are obtained from a model-based approach [11], such that the visco-elastic torque τ_{VIM} is calculated as

$$\tau_{VIM}(t) = K(t)(\theta_{set}(t) - \theta(t)) - B(t)\dot{\theta}(t) \quad (1)$$

with $\theta(t)$ and $\dot{\theta}(t)$ the joint angle and angular velocity of the prosthesis. It is known that the visco-elastic impedance model (*ViscImp*) describes the general behavior of the joint

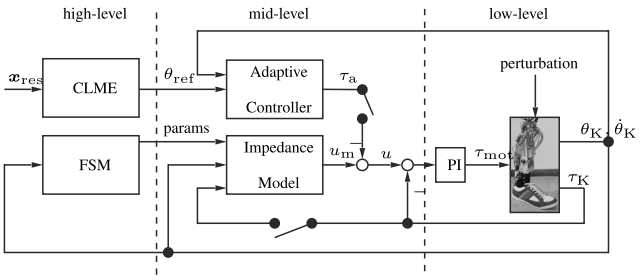

Fig. 1. Concept of the proposed bio-inspired control scheme. High-level control includes estimation of the reference trajectory with Complementary Limb Motion Estimation (CLME) [19] and provision of control parameters with a FSM. Mid-level control includes the impedance controller and, facultative, the adaptive controller. Low-level control includes a PI force controller which generates the required knee joint moment [11].

reasonably well, although it does not reflect the underlying physiological mechanisms [8]. Therefore, neuromusculoskeletal models have been proposed that include the intrinsic muscle visco-elasticity and the reflexive feedback from muscle spindles (MS) and Golgi tendon organs (GTO) [21]. The reflexive feedback mechanisms have been shown to allow for precise movements despite perturbations [22]. The neuromusculoskeletal joint moment $\tau_{NIM}(t)$ is composed of the intrinsic and the reflexive moment $\tau_i(t)$ and $\tau_r(t)$:

$$\tau_{NIM}(t) = \tau_i(t) + \tau_r(t) \quad (2)$$

The intrinsic component is obtained similar to the *ViscImp* in eq. (1), using a proportional gain $k_i(t)$ and a damping parameter $b_i(t)$:

$$\tau_i(t) = k_i(t)(\theta_{set}(t) - \theta(t)) - b_i(t)\dot{\theta}(t) \quad (3)$$

The reflexive component is delayed by $T_d = 40$ ms and obtained with an additional stiffness $k_{MS}(t)$ and damping $b_{MS}(t)$ of the muscle spindles and the Golgi tendon feedback gain $k_{GTO}(t)$ that generates positive force feedback:

$$\tau_r(t) = \big(k_{MS}(t)(\theta_{set}(t) - \theta(t - T_d)) - b_{MS}(t)\dot{\theta}(t - T_d) + k_{GTO}(t)\ \tau_{NIM}(t - T_d)\big) \cdot h_{act}(t). \quad (4)$$

Hereby, the activation dynamics $h_{act}(t)$ translate the excitation to the activation signal and are modeled as a second-order filter with natural frequency $\omega_n = 4.4\pi rads^{-1}$ and relative damping $\beta = 0.7$ [23]. Compared to the *ViscImp*, the bio-inspired *NeurImp* comes at the cost of an increased number of free parameters that have to be tuned.

A FSM is used to set the appropriate parameters for each of the four states defined (see table I). Stance phase is divided into (1) early-mid stance and (2) late stance, whereas swing phase is subdivided into (3) swing flexion and (4) late swing. Transition conditions as well as parameters for the *ViscImp* have been validated in former experiments [11]. Angular velocity serves to avoid uncontrolled backward transitions e.g. from 2 to 1 while standing. For now, parameters for the *NeurImp* were found by manual tuning.

B. Human Model Reference Adaptive Control

In this section, a Human Model Reference Adaptive Controller (*HuMRAC*; [24], [25]) is designed based on models

TABLE I
PARAMETERS FOR VISCO-ELASTIC AND NEUROMUSCULOSKELETAL IMPEDANCE MODEL FOR ALL FOUR STATES. $K, B, \theta_{\mathrm{SET}}$ AS WELL AS THE TRANSITION CONDITIONS WERE OBTAINED FROM AND VALIDATED IN [11]. PARAMETERS FOR *NeurImp* WERE FOUND BY MANUAL TUNING. PARAMETERS ARE IDENTICAL FOR ALL THREE SUBJECTS

phase	stance		swing	
state	1	2	3	4
K (Nm/°)	3.84	2.09	1.40	0.18
B (Nms/°)	0.02	0	0	0.2
k_{i} (Nm/°)	2.09	1.4	1.4	0.18
b_{i} (Nms/°)	0.02	0.02	0.04	0.02
k_{MS} (Nm/°)	1.92	1.05	0	0
b_{MS} (Nms/°)	0.01	0.02	0	0
k_{GTO} (-)	0.1	0	0.1	0
θ_{set} (°)	8	7	20	20
transition condition θ (°)	>10	>20	>50	<15
transition condition $\dot{\theta}$ (°/s)	>5.7	>5.7	<0	-

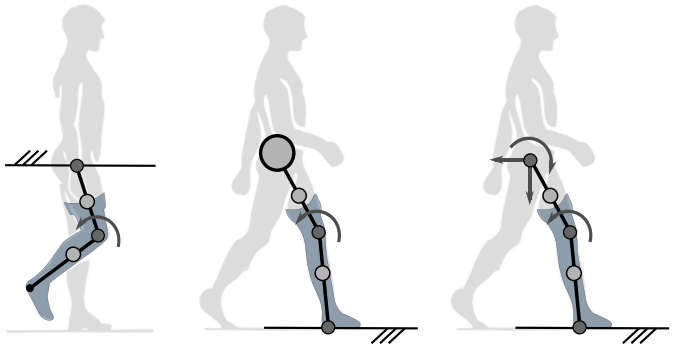

Fig. 2. Multi-segmented leg models used to design the adaptive controller *HuMRAC* and to simulate prosthetic stance phase. (a) *HuMRAC* swing phase: double pendulum. (b) *HuMRAC* stance phase: double inverted pendulum with HAT mass. (c) Simulation stance phase: double inverted pendulum with feedforward physiological hip forces and moment. In models (a) and (b), the knee joint is actuated using the *NeurImp*. In model (c), either of the two impedance controllers is used.

of human walking dynamic. In these models, either of the two physiological paradigms described in II-A can be used to modulate knee joint impedance.

1) System Dynamics: To describe the dynamics of prosthetic gait, two different models are used: a double pendulum during swing phase (see Fig. 2.a) and a double inverted pendulum during stance phase (see Fig. 2.b). The two segments represent the residual limb and the transfemoral prosthesis. During swing, the segments rotate around the hip and the prosthetic knee joint, respectively. During stance, they rotate around the knee and the passive ankle joint, which is modeled as a pivot point on the ground because the ANGELAA prosthesis does not possess an actuated ankle [11]. The interaction between the leg and the head-arms-trunk unit (HAT) is modeled as a point mass at the height of the hip. During the entire gait cycle, only the knee joint is actuated. Physiological masses, inertias and lengths for the leg segments, scaled to body height $h = 1.8$m and mass $m = 85kg$, are obtained from Winter [26] whereas properties of the prosthesis are obtained from the CAD model of our ANGELAA prosthesis. For each time step, the non-linear human reference models for stance and swing phase are linearized around the current state, i.e. joint positions and velocities [27]. These linearized models can be expressed in state-space representation:

$$\dot{\boldsymbol{x}}_{\mathrm{m}}(t) = \mathbf{A}_{\mathrm{m}}(t)\boldsymbol{x}_{\mathrm{m}}(t) + \boldsymbol{b}_{\mathrm{m}}(t)\tau_{\mathrm{m}}(t), \tag{5}$$

$$\boldsymbol{y}_{\mathrm{m}}(t) = \mathbf{C}_{\mathrm{m}}\boldsymbol{x}_{\mathrm{m}}(t), \tag{6}$$

with the system matrices $\mathbf{A}_{\mathrm{m}}(t) \in \mathbb{R}^{4x4}$, $\boldsymbol{b}_{\mathrm{m}}(t) \in \mathbb{R}^{4\times1}$ and $\mathbf{C}_{\mathrm{m}} = \mathbf{I} \in \mathbb{R}^{4\times4}$, the bounded human model reference input $\tau_{\mathrm{m}}(t)$ containing the knee moment, the model state vector $\boldsymbol{x}_{\mathrm{m}}(t) = \left(\theta_{\mathrm{t}}(t)\ \theta_{\mathrm{s}}(t)\ \dot{\theta}_{\mathrm{t}}(t)\ \dot{\theta}_{\mathrm{s}}(t)\right)^T$ containing absolute thigh and shank angles $\theta_{\mathrm{t}}(t)$ and $\theta_{\mathrm{s}}(t)$ and their respective velocities, and the model output $\boldsymbol{y}_{\mathrm{m}}(t) = \boldsymbol{x}_{\mathrm{m}}(t)$. To obtain the desired closed-loop dynamics of the system, $\tau_{\mathrm{m}}(t)$ is replaced with either the *NeurImp* (eq. (2)) or the *ViscImp* (eq. (1)). Using exemplarily the latter, this results in:

$$\begin{aligned}\dot{\boldsymbol{x}}_{\mathrm{m}}(t) &= \mathbf{A}_{\mathrm{m}}(t)\boldsymbol{x}_{\mathrm{m}}(t) + \boldsymbol{b}_{\mathrm{m}}(t)\left(K(t)\theta_{\mathrm{set}}(t) - \boldsymbol{w}(t)\boldsymbol{x}_{\mathrm{m}}(t)\right)\\ &= \mathbf{A}(t)\boldsymbol{x}_{\mathrm{m}}(t) + \boldsymbol{b}(t)u_{\mathrm{m}}(t),\end{aligned} \tag{7}$$

with $u_{\mathrm{m}}(t) = K(t)\theta_{\mathrm{set}}(t)$ the input of the ideal closed-loop dynamics, $\boldsymbol{w}(t) = \left(K(t)\ -K(t)\ B(t)\ -B(t)\right)$ as well as $\mathbf{A}(t) = \mathbf{A}_{\mathrm{m}}(t) - \boldsymbol{b}_{\mathrm{m}}(t)\boldsymbol{w}(t)$ and $\boldsymbol{b}(t) = \boldsymbol{b}_{\mathrm{m}}(t)$.

2) Model Reference Adaptive Controller: To account for uncertainties, we augment the ideal system dynamics (7) using an unknown vector function $\boldsymbol{k}_{\mathrm{u}}(t)$:

$$\dot{\boldsymbol{x}}(t) = (\mathbf{A}(t) + \boldsymbol{b}(t) \otimes \boldsymbol{k}_{\mathrm{u}}(t))\boldsymbol{x}(t) + \boldsymbol{b}(t)u(t). \tag{8}$$

The uncertainty term $\boldsymbol{k}_{\mathrm{u}}(t)$ captures unmodeled effects such as differences in physiology or differences between sound and prosthetic legs.

With the objective to suppress $\boldsymbol{k}_{\mathrm{u}}(t)$ in the actual closed-loop dynamics (8) such that they match the ideal closed-loop dynamics (7), the control law is defined as

$$u(t) = u_{\mathrm{m}}(t) - \widehat{\boldsymbol{k}}_{\mathrm{u}}^T(t)\boldsymbol{x}(t). \tag{9}$$

The adaptive term $\widehat{\boldsymbol{k}}_{\mathrm{u}}(t)$ is an estimate of $\boldsymbol{k}_{\mathrm{u}}(t)$ and $\widehat{\boldsymbol{k}}_{\mathrm{u}}^T(t)\boldsymbol{x}(t)$ equals the adaptive knee joint moment $\tau_{\mathrm{a}}(t)$. Substituting (9) in (8) yields the closed-loop system dynamics:

$$\begin{aligned}\dot{\boldsymbol{x}}(t) &= (\mathbf{A}(t) - \boldsymbol{b}(t) \otimes \widetilde{\boldsymbol{k}}_{\mathrm{u}}(t))\boldsymbol{x}(t) + \boldsymbol{b}(t)u_{\mathrm{m}}(t),\\ \boldsymbol{y}(t) &= \mathbf{C}(t)\boldsymbol{x}(t),\end{aligned} \tag{10}$$

with the actual states $\boldsymbol{x}(t)$, the actual plant output $\boldsymbol{y}(t)$ and the output matrix $\mathbf{C}(t) \in \mathbb{R}^{4x4}$, as well as with the parametric estimation error $\widetilde{\boldsymbol{k}}_{\mathrm{u}}(t) = \widehat{\boldsymbol{k}}_{\mathrm{u}}(t) - \boldsymbol{k}_{\mathrm{u}}(t)$.

The objective of the *HuMRAC* is to find an adaptation law for $\widehat{\boldsymbol{k}}_{\mathrm{u}}(t)$ such that the plant dynamics $\boldsymbol{y}(t)$ track the bounded piecewise-continuous model reference $\boldsymbol{y}_{\mathrm{m}}(t)$. This is in line with physiology where the impedance of the human leg is adjusted to minimize the error between the actual and the desired movement while minimizing the actuation effort [18]. Given a desired reference knee joint trajectory $\theta_{\mathrm{ref}}(t)$ and a desired thigh angle $\theta_t(t)$, the model state vector can be rewritten as $\boldsymbol{x}_{\mathrm{m}}(t) = \left(\theta_{\mathrm{t}}(t)\ \theta_{\mathrm{t}}(t) - \theta_{ref}(t)\ \dot{\theta}_{\mathrm{t}}(t)\ \dot{\theta}_{\mathrm{t}}(t) - \dot{\theta}_{\mathrm{ref}}(t)\right)^T$. A cost function $J(t)$ which includes the tracking error $\boldsymbol{e}(t) =$

$\boldsymbol{x}_{\mathrm{m}}(t) - \boldsymbol{x}(t)$ and the control effort $E(t)$ can therefore be used to derive the requirements for a bio-inspired adaptation law:

$$J(t) = \boldsymbol{e}^T(t)\boldsymbol{e}(t) + \gamma\, E(t), \tag{11}$$

with the tunable gain γ. The effort term can be chosen as a quadratic function of the change in the adaptive knee moment such that $E(t) = \dot{\tau}_{\mathrm{a}}(t)^2$. Minimizing $J(t)$ with respect to $\dot{\tau}_{\mathrm{a}}(t)$ allows to minimize the effort related to undesired changes in the torque profile and results in:

$$\dot{\tau}_{\mathrm{a}}(t) = -\frac{1}{\gamma}\boldsymbol{e}^T(t)\frac{\mathrm{d}\boldsymbol{e}(t)}{\mathrm{d}\dot{\tau}_{\mathrm{a}}(t)}, \quad \text{with} \tag{12}$$

$$\frac{\mathrm{d}\boldsymbol{e}(t)}{\mathrm{d}\dot{\tau}_{\mathrm{a}}(t)} = -\int_0^t \exp(\mathbf{A}(t-\bar{t}))\boldsymbol{b}\bar{t}\mathrm{d}\bar{t} \tag{13}$$

the integral over time $\bar{t}$. Thus, the change of the adaptive moment $\dot{\tau}_{\mathrm{a}}(t)$ must be proportional to the kinematic error $\boldsymbol{e}(t)$ and the tunable gain γ^{-1} which weighs the contribution of $E(t)$ and $\boldsymbol{e}(t)$ in the cost function (11).

A possible update law for the parametric estimate $\widehat{\boldsymbol{k}}_{\mathrm{u}}(t)$ proposed in [28] is

$$\dot{\widehat{\boldsymbol{k}}}_{\mathrm{u}}(t) = -\Gamma\boldsymbol{x}(t)\boldsymbol{e}^T(t)\mathbf{V}\mathbf{P}\boldsymbol{b}, \tag{14}$$

with $\Gamma \in \mathbb{R}^+$ the adaptation gain used to regulate how fast the adaptation takes place, $\mathbf{P} \geq 0 \in \mathbb{R}^{4x4}$ the forgetting matrix used for tuning, and $\mathbf{V} = \mathbf{V}^T \succ 0 \in \mathbb{R}^{4x4}$ the solution to the algebraic Lyapunov equation for arbitrary $\mathbf{Q} = \mathbf{Q}^T \succ 0$:

$$\mathbf{A}^T\mathbf{V}\mathbf{P} + \mathbf{V}\mathbf{P}\mathbf{A} = -\mathbf{Q}. \tag{15}$$

Equation (9) fulfills the requirements for the control law derived from the cost function (11).

Due to the two different models for stance (st) and swing (sw) phase, it is necessary to implement a fading strategy for the adaptive moment τ_{a}:

$$\tau_{\mathrm{a}} = f_1(\theta_{\mathrm{K}})\tau_{\mathrm{a}}^{\mathrm{st}} + f_2(\theta_{\mathrm{K}})\tau_{\mathrm{a}}^{\mathrm{sw}}. \tag{16}$$

The weighting factors $f_1(\theta_{\mathrm{K}})$ and $f_2(\theta_{\mathrm{K}})$ are chosen as linear functions of the knee joint angle θ_{K}. Within $\pm 2°$ around the defined state transition angle (compare table I), one factor increases from 0 to 1 while the other factor decreases from 1 to 0.

For *NeurImp*, a reference model (eq. 7) and a control law (eq. 9 and 14) have been derived accordingly.

The proposed control strategy is not conservative and can be applied to the given linearized time-variant system only based on the strict assumption that the system dynamics and the control dynamics act on different time scales. The control is reset during each fading between stance and swing phase, which limits the variation range of the system non-linear dynamics in time.

III. Simulation

While the *ViscImp* has already been used to control a prosthetic leg [11], the objective of the simulation was to evaluate whether the *NeurImp* and the *HuMRAC* have as well the potential to safely control an active knee exoprosthesis and to realize quasi-physiological dynamics as well as good tracking properties. Therefore, two simulations of stance phase were performed.

A. Validation of Control Concept

1) Properties of NeurImp: For a preliminary evaluation of the *NeurImp* properties, in particular to investigate whether physiological kinematics can be realized, a forward simulation of unperturbed prosthetic stance phase was implemented using Matlab R2014a (The Mathworks, Natwick, USA). The model of stance phase dynamics described in section II-B1 was adapted (see Fig. 2.c): the interaction between the leg and the upper body was modeled with hip forces and moments obtained from the gait analysis of an unimpaired male subject during steady level-ground walking. This ensures that the physiological interaction with the upper body is always maintained while testing the *NeurImp*. Furthermore, this choice emphasizes the objective to restore a physiological gait pattern using the control strategies presented here. The simulation of stance phase lasted for 1.11s, which corresponds to the average duration at a walking speed of 2.7km/h, used in the experiments. Initial thigh and shank angles and velocities were chosen to match the physiological gait data at heel strike. Transition conditions for the simulation were taken from table I. All gains, however, were scaled by a factor of five to allow for a stable simulation. To compare the performance of the *NeurImp* with the *ViscImp*, the simulation was as well conducted with the latter (see eq. (2)).

2) Performance of HuMRAC: For a preliminary evaluation of the adaptive controller's tracking and dynamic performance, sum-of-sinusoids moment perturbations $\tau_{\mathrm{pert}}(t)$ (amplitude 15Nm, maximum resultant amplitude 36Nm, maximum frequency 100Hz) around the knee joint were added to the forward simulation described in section III-A1. These perturbations represent lumped uncertainties when walking with the prosthesis. In the first simulation, the *NeurImp* knee moment $\tau_{\mathrm{NIM}}(t)$ and the additional perturbation moment $\tau_{\mathrm{pert}}(t)$ acted around the knee joint, while the adaptive control was turned off:

$$\tau_{\mathrm{K}}(t) = \tau_{\mathrm{NIM}}(t) + \tau_{\mathrm{pert}}(t), \tag{17}$$

with the resulting simulated knee joint moment $\tau_{\mathrm{K}}(t)$. In the second simulation, the adaptive control was turned on and the adaptive moment $\tau_{\mathrm{a}}(t)$ was generated:

$$\tau_{\mathrm{K}}(t) = \tau_{\mathrm{NIM}}(t) + \tau_{\mathrm{pert}}(t) + \tau_{\mathrm{a}}(t). \tag{18}$$

A meaningful initial value for $\widehat{\boldsymbol{k}}_{\mathrm{u}}(0)$ in (9) and (14) was found with manual tuning. The adaptive controller had to track a reference knee angle trajectory $\theta_{\mathrm{ref}}(t)$ which equaled the recorded physiological knee angle $\theta_{\mathrm{phys}}(t)$. Please note that the reference model used to design the *HuMRAC* (Fig. 2.b) and the model used in the simulation (Fig. 2.c) with additional knee moment perturbations) differ and, thus, should partly reflect the discrepancy between the model assumed by the controller and the actual plant. To compare the two impedance models, the simulation was also conducted with *ViscImp*, i.e. τ_{NIM} was replaced by τ_{VIM} in equations (17) and (18).

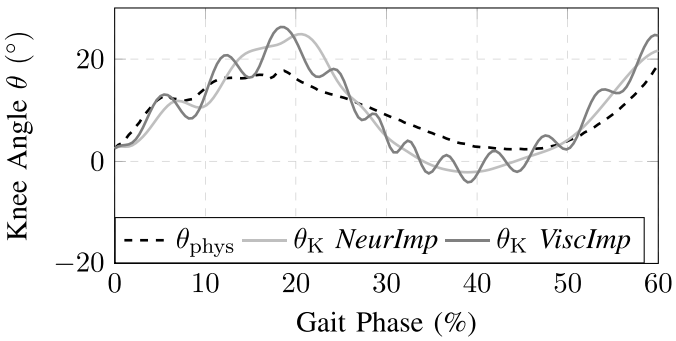

Fig. 3. Forward simulation of *unperturbed* stance phase using the *NeurImp* (light gray) and the *ViscImp* (gray): simulated $\theta_K(t)$ compared to recorded physiological knee joint angle $\theta_{phys}(t)$ (black dashed).

B. Data Processing and Analysis

To evaluate the performance of the controllers, the root mean square error (RMSE) was calculated by comparing each j-th sample of the recorded physiological knee angle $\theta_{j,\text{phys}}$ with its simulated counterpart $\theta_{j,K}$:

$$\text{RMSE} = \sqrt{\frac{1}{N}\sum_{j=1}^{N}(\theta_{j,\text{phys}}^2 - \theta_{j,K}^2)}, \tag{19}$$

with N the total number of samples.

C. Results

1) Properties of NeurImp: Figure 3 shows the two simulated $\theta_K(t)$ and the recorded physiological knee joint trajectory $\theta_{phys}(t)$.

The RMSE for these simulations can be found in the top row of table II.

2) Performance of HuMRAC: Figure 4 (top panels) shows the simulated knee joint angle $\theta_K(t)$ for *NeurImp* and *ViscImp*, and the desired reference knee joint angle $\theta_{ref}(t) = \theta_{phys}(t)$. The RMSE for all conditions are listed in table II.

Figure 4 also shows the total simulated $\tau_K(t)$ using *NeurImp* (second row) and *ViscImp* (third row), the reference $\tau_{ref}(t)$, the perturbation $\tau_{pert}(t)$ and the respective adaptive $\tau_a(t)$ knee joint moment.

D. Discussion

1) Properties of NeurImp: In the simulation, the *NeurImp* allows for a fair match between simulated and physiological joint angle trajectories, despite a small time delay at stance onset and increased knee flexion and extension peaks which are accompanied by large position errors. Still, the RMSE is below 4.5°, which overlaps with the smallest perceivable position error range for lower limbs in unimpaired subjects [29]. The *ViscImp* results in a slightly smaller position error but shows a more oscillatory and, therefore, less physiological behavior.

2) Performance of HuMRAC: The simulations of a perturbed stance phase reveal that the *HuMRAC* allows to successfully track a physiological reference trajectory. The *HuMRAC* reduces the RMSE by 96% to less than 0.3° for both impedance models. With the *NeurImp*, despite the large perturbation moment with an amplitude of 36Nm, the adaptive control compensates for the disturbance such that the resulting knee joint moment shows an almost physiological profile in the range of –85 to 49 Nm. With the *ViscImp*, the resultant torque profile (–88 to 34 Nm) improves in smoothness and amplitude compared to the perturbed torque profile (–178 to 238 Nm). For perturbed stance as well, the *ViscImp* shows a more oscillatory behavior and larger RMSE compared to the *NeurImp*. The *HuMRAC* seems to restore physiological knee joint dynamics while maintaining physiological interaction forces and moments at the hip joint. Although a model-based reference adaptive controller is in general designed for slowly varying dynamics, in the simulation, the *HuMRAC* converges towards the reference trajectory within only 0.1s. This suggests that the model dynamics used to design the *HuMRAC* closely match the actual dynamics of the simulated plant. Still, the different physiology of unimpaired and amputee gait, e.g. inter-subject variability in gait patterns, leg properties and control are neglected in the simulation. Furthermore, the reference trajectory and the force profiles used are based on feed-forward physiological gait data. Thus, more complex non-linear human dynamic models, and amputee gait data as input might improve the simulation.

TABLE II
RMSE BETWEEN THE ACTUAL θ_K AND THE PHYSIOLOGICAL REFERENCE θ_{REF} KNEE JOINT ANGLE DURING THE UNPERTURBED AND THE PERTURBED STANCE PHASE SIMULATION. THE LAST COLUMN SHOWS THE PERCENTAGE CHANGE OF THE RMSE: IF $\Delta\% < 0$, IN CONTROL MODE 2 THE SIMULATED KNEE ANGLE TRAJECTORY DEVIATED LESS FROM THE REFERENCE TRAJECTORY COMPARED TO CONTROL MODE 1

simulation	RMSE (°)		Δ%
unperturbed	*ViscImp*	*NeurImp*	
	4.23	4.33	+2.31
perturbed	*NeurImp*	*NeurImp* + *HuMRAC*	
	5.30	0.19	-96.42
perturbed	*ViscImp*	*ViscImp* + *HuMRAC*	
	7.55	0.26	-96.57

IV. PILOT EXPERIMENT WITH HUMAN SUBJECTS

The objective of the pilot experiment was to assess the general feasibility of the *NeurImp* for variable impedance control as well as the performance of the adaptive controller *HuMRAC* in a real-world application. Furthermore, neuromusculoskeletal was compared to variable visco-elastic impedance control.

A. Setup and Protocol

Two unimpaired subjects S1 and S2 (age 26 and 30 years, height both 178cm, weight 85 and 60 kg, one male, one female) and one amputee subject A (46 years, 186cm; 75 kg, male; knee exarticulation, right, 2 years post-amputation)

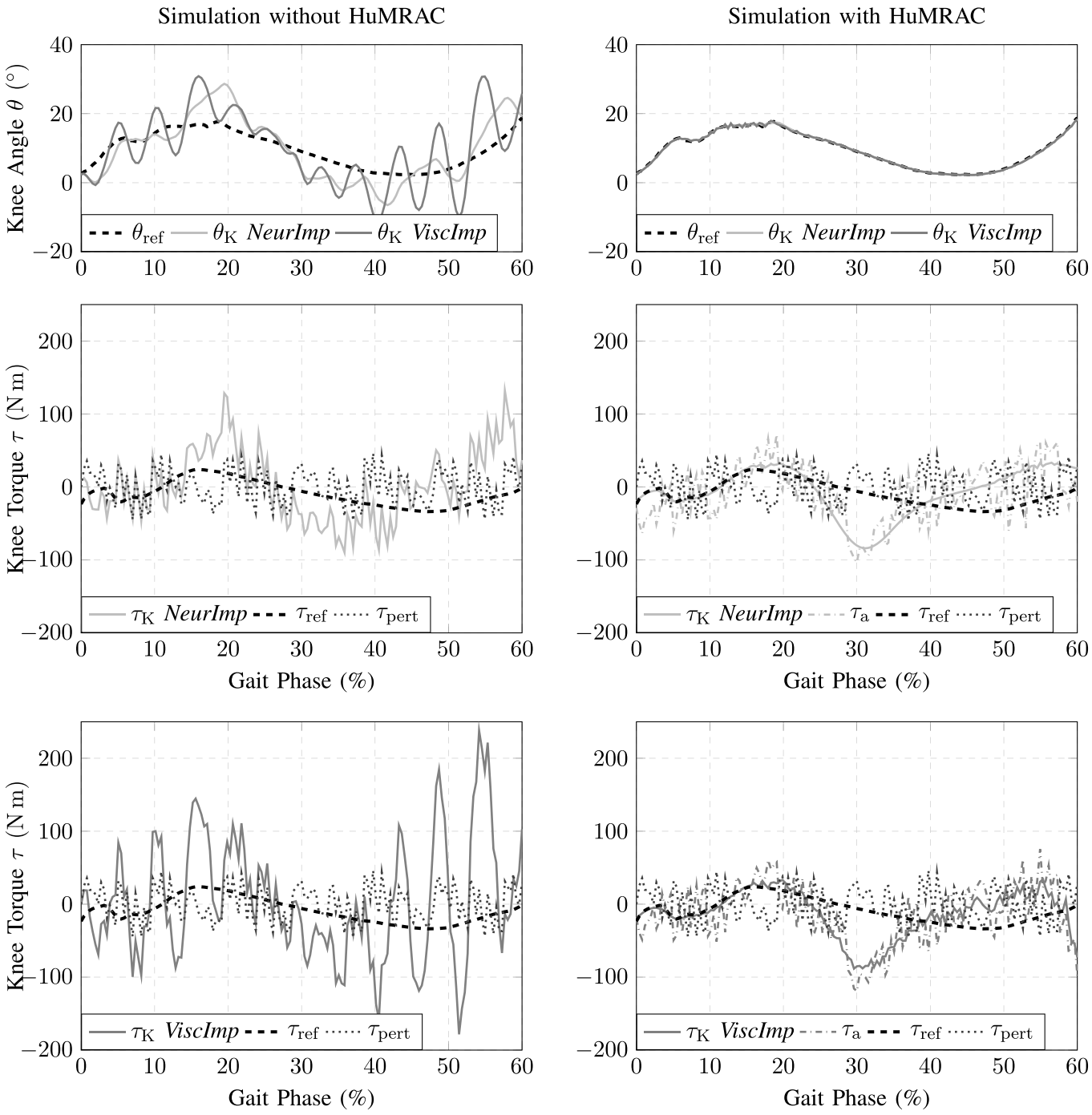

Fig. 4. Forward simulation of *perturbed* stance phase using the *NeurImp* (second row) and the *ViscImp* (third row) without (left panels) and with *HuMRAC* (right panels). First row: Simulated $\theta_K(t)$ and physiological reference $\theta_{ref}(t) = \theta_{phys}(t)$ knee joint trajectory. Second and third row: Simulated $\tau_K(t)$ and physiological reference $\tau_{ref}(t) = \tau_{phys}(t)$ knee joint moment as well as perturbation $\tau_{pert}(t)$ and adaptive $\tau_a(t)$ knee joint moment.

participated in the pilot experiment. Subjects wore the actuated ANGELAA prosthetic leg on the right side. The two unimpaired subjects connected the prosthesis using a fake socket and wore a TwinShoe (DARCO, Raisting, Germany) on the left side to compensate for different leg lengths (see Fig. 5, right). The prosthesis was controlled in real-time using Matlab Simulink R2013b (The Mathworks, Natick, MA, USA) running on a xPC Target Real-time computer (Speedgoat GmbH, Liebefeld, Switzerland) at 1KHz. To ensure the participants' safety, electrical and software range limitations as well as manual emergency stop switches were implemented. For a quantitative analysis, the prosthetic knee joint angle was measured using a 17 bit absolute encoder (Netzer Precision Motion Sensors Ltd., Misgav, Israel). To measure gait kinematics that were required for the adaptive controller, a customized wearable sensor setup including six inertial measurement units (IMU; 3Space Sensor, Yost Engineering, USA) was used. Data was acquired

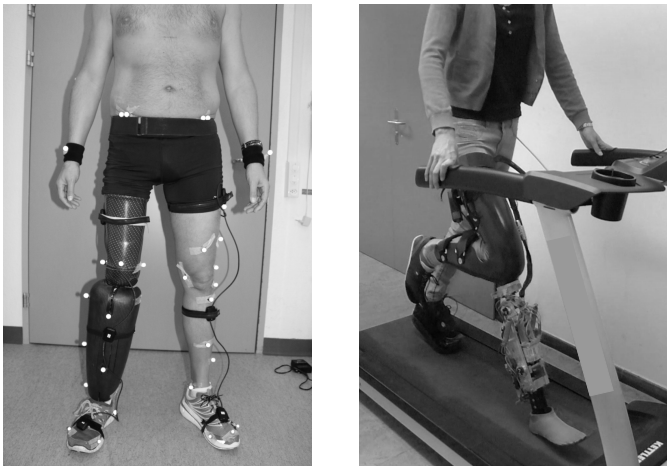

Fig. 5. Left: Amputee subject wearing the IMU sensor setup on both legs and the ANGELAA prosthesis. Right: Unimpaired subject walking on the treadmill.

TABLE III
IN EACH OF THE THREE CONDITIONS, TWO CONTROL MODES WERE COMPARED. THE TWO IMPEDANCE MODELS *ViscImp* AND *NeurImp* WERE TESTED ALONE OR IN COMBINATION WITH THE ADAPTIVE CONTROLLER *HuMRAC*

condition	control mode 1	control mode 2
1	*ViscImp*	*NeurImp*
2	*NeurImp*	*NeurImp + HuMRAC*
3	*ViscImp*	*ViscImp + HuMRAC*

with the real-time computer through a PCI serial board with eight RS-232 serial ports (Quatech ESC-100-D9; Quatech, Ottawa, USA). The IMUs were placed on both the sound and the prosthetic foot, shank and thigh. Static calibration prior to the experiment was conducted to align the sensor coordinate systems with the body planes. The IMU inclination angle was estimated both from gyroscope as well as from accelerometer measurements. For accurate estimations of joint and segment angles as well as angular velocities, the two estimates were fused using a complementary filter [30].

Subjects participated voluntarily. The experiment was approved by the Ethics Committee of the Canton of Zurich. A physiotherapist was present and ready to give support if necessary.

To familiarize with the prosthesis, subjects walked on the treadmill (zebris Medical GmbH, Isny, Germany) for at least ten minutes and tested the *ViscImp* as well as the *NeurImp* without the adaptive controller. As soon as they felt comfortable with the setup, in each of the three conditions that are listed in table III, two control modes were compared. Each of the control modes was tested for at least two minutes at a walking speed of 2.7km/h. Throughout the experiment, subjects were allowed to hold the handrails to keep balance. Resting breaks were allowed whenever required.

In conditions that included the adaptive controller, the reference trajectory $\theta_{\text{ref}}(t)$ was instantaneously calculated from the user's sound leg movements $\boldsymbol{x}_{\text{res}}$, using Complementary Limb Motion Estimation (CLME) (see Fig. 1). CLME exploits the strong inter-joint coupling of human locomotion to deduce the intended motion of the prosthetic leg from residual body motion [19]. For that purpose, off-line, a general neural network was trained with gait data from an unimpaired subject walking with the ANGELAA prosthesis, which was controlled with a standard hierarchical state controller (unpublished work). Shank and thigh segment as well as knee joint angles and velocities of the sound side served as predictors $\boldsymbol{x}_{\text{res}}$. The average physiological knee joint trajectory $\theta_{\text{phys}}(t)$ that was synchronized with the gait cycle of the state controller served as target for the prediction.

B. Data Processing and Analysis

Prior to the analysis, the data was downsampled to 250Hz. To segment the data, heel strike (HS) and toe off (TO) were detected using the foot segment angular velocity measured with the IMU sensor setup [31].

To objectively evaluate the different control modes, the mean and standard deviation of the RMSE between the actual knee angle trajectory $\theta_{\text{K}}(t)$ measured with the encoder and the mean physiological knee joint trajectory $\theta_{\text{phys}}(t)$ was calculated (see III-B).

To subjectively evaluate the different control modes, subjects answered the following questions: (A) "How difficult is the stance-to-swing transition?" (B) "Do you feel constrained by the adaptive controller?" (C) "How natural is the perception of control mode 2 compared to control mode 1?" (D) "Which of the two do you prefer?"

C. Results

Table IV shows the RMSE between the actual $\theta_{\text{K}}(t)$ and the mean physiological knee joint trajectory $\theta_{\text{phys}}(t)$ for all three subjects and all conditions during stance phase.

In condition 1, the RMSE increased for all subjects when walking with the *NeurImp* compared to when walking with the *ViscImp*. In condition 2, the RMSE decreased up to 54% for all three subjects when combining the *NeurImp* with the adaptive controller. In condition 3, the RMSE decreased for S1 and A when combining the *ViscImp* with the adaptive controller. For S2, the RMSE increased slightly.

Figure 6 exemplarily shows the prosthesis' knee joint angle for all three subjects in condition 1 in which the two impedance models are compared and the *HuMRAC* is inactive. Table V lists the subjects' answers to the four questions.

D. Discussion

The three subjects preferred the *NeurImp* because it facilitated the stance-to-swing transition and felt more natural than the visco-elastic impedance model. This may be due to increased damping compared to the *ViscImp*, which is well visible in the simulation. However, this positive subjective evaluation of the *NeurImp* compared to the *ViscImp* is not in line with the increased deviation from the physiological knee angle which has already been observed in the simulation.

Furthermore, the three subjects preferred walking with the *HuMRAC* over walking without the *HuMRAC*. This positive

TABLE IV
MEAN AND STANDARD DEVIATION OF THE RMSE BETWEEN THE ACTUAL $\theta_{\mathrm{K}}(t)$ AND THE PHYSIOLOGICAL $\theta_{\mathrm{PHYS}}(t)$ KNEE JOINT ANGLE DURING STANCE PHASE FOR ALL SUBJECTS AND ALL CONDITIONS. THE LAST COLUMN SHOWS THE PERCENTAGE CHANGE OF THE RMSE BETWEEN THE CONTROL MODES: IF $\Delta\% < 0$, IN CONTROL MODE 2 THE ACTUAL KNEE ANGLE TRAJECTORY DEVIATED LESS FROM THE PHYSIOLOGICAL REFERENCE COMPARED TO CONTROL MODE 1

subject	RMSE (std) (°)		$\Delta\%$
condition 1	*ViscImp*	*NeurImp*	
S1	4.95 (0.53)	5.57 (0.51)	+12.53
S2	4.06 (0.38)	4.17 (0.26)	+2.8
A	4.89 (1.49)	5.88 (0.69)	+20.154
condition 2	*NeurImp*	*NeurImp + HuMRAC*	
S1	7.32 (0.64)	3.36 (0.76)	-54.12
S2	4.17 (0.45)	3.86 (0.39)	-7.37
A	6.06 (0.34)	4.87 (0.63)	-19.64
condition 3	*ViscImp*	*ViscImp + HuMRAC*	
S1	5.41 (0.62)	3.35 (0.58)	-38.12
S2	3.21 (0.40)	3.49 (0.34)	+8.86
A	4.64 (0.34)	4.54 (0.58)	-2.17

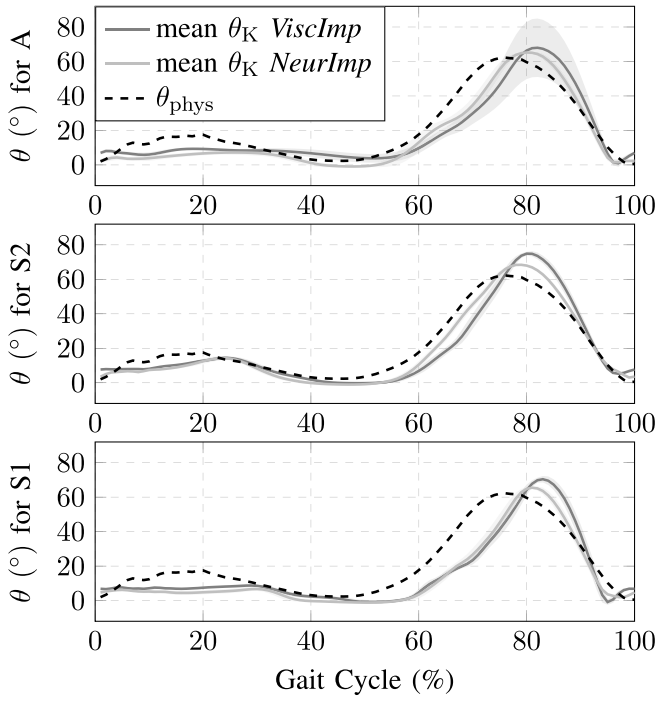

Fig. 6. Prosthesis' knee joint angle $\theta_{\mathrm{K}}(t)$ (mean±std) for all three subjects. The gray and the light gray line show the results for the *ViscImp* and the *NeurImp*, respectively. The black dashed line depicts the mean physiological reference angle $\theta_{\mathrm{phys}}{\triangleright}t{\triangleleft}$.

subjective evaluation supports the finding that the movement resembled the physiological reference more closely, with only one exception for unimpaired subject S2 walking with the visco-elastic impedance control. However, compared to the simulation, within one gait cycle the *HuMRAC* did not succeed to converge as close towards the desired trajectory. On the one hand, the reference trajectory used in the experiments has been estimated on-line using CLME, and is, therefore, influenced by estimation inaccuracies due to sensor movements and positioning as well as different gait patterns. On the other hand, stability limitations of the series elastic actuation required a reduction of the adaptation gain Γ compared to the simulation. Although stiff position control is not desired as it does not correspond to the physiological knee joint behavior, fine-tuning of the *HuMRAC* parameters may allow for a better compromise between stability and performance. Given the large standard deviations of the RMSE and the disputability of subjective evaluations, the experiment should be repeated with more subjects. Still, the applicability and repeatability of both control concepts has been confirmed.

TABLE V
EVALUATION OF THE QUESTIONNAIRE. SUBJECTS ANSWERED QUESTIONS (A)–(C) ON A SCALE FROM 1 TO 5. (A) SWING-TO-STANCE TRANSITION, 1: TOO EASY, 5: TOO DIFFICULT; (B) CONSTRAINED BY *HuMRAC*, 1: NOT AT ALL, 5: ABSOLUTELY; (C) COMPARISON OF NATURAL PERCEPTION, 1: MUCH WORSE, 5: MUCH BETTER. IN QUESTION (D), SUBJECTS STATED WHICH CONTROL MODE THEY PREFERRED

	subject	A	B	C	D
ViscImp vs *NeurImp*	S1	4 vs 3	-	4	*NeurImp*
	S2	3 vs 3	-	4	*NeurImp*
	A	2 vs 3	-	4	*NeurImp*
NeurImp vs *NeurImp + HuMRAC*	S1	2 vs 2	1	3	*HuMRAC*
	S2	3 vs 1	1	4	*HuMRAC*
	A	n/a	2	3	*HuMRAC*
ViscImp vs *ViscImp + HuMRAC*	S1	4 vs 2	2	4	*HuMRAC*
	S2	4 vs 1	2	4	*HuMRAC*
	A	4 vs 2	n/a	4	*HuMRAC*

V. CONCLUSION AND OUTLOOK

In this work, a bio-inspired control approach to modulate and to adapt dynamics of an active knee exoprosthesis has been presented.

In the simulation, the *NeurImp* performed well despite the inherent time delay and the positive moment feedback. Compared to the well-known and prevalent *ViscImp*, position errors increased only slightly. When adding the adaptive controller to either of the impedance controllers, the simulations revealed that during stance phase accurate position tracking as well as physiological knee moment generation are achieved.

In the pilot experiment like in the simulation, the *NeurImp* performed well despite increased position errors compared to the *ViscImp*. Nevertheless, the three subjects preferred the *NeurImp* and reported a more natural behavior of the prosthesis which is in line with the simulation. Despite being less sharp than in the simulations, the *HuMRAC* reduced the angle deviation below the smallest perceivable position error range for young unimpaired subjects [29]. The subjects preferred walking with the *HuMRAC* switched on and reported a facilitated stance-to-swing transition. The pilot experiment

did not reveal different effects for amputee and unimpaired subjects.

In the future, three main improvements for the controllers are conceivable. First, classical model-based reference adaptive control assumes a linear plant and a linear reference model. However, human gait dynamics are non-linear and time-variant. Therefore, more sophisticated adaptive control schemes could be investigated [32]. Second, the reference model could be customized for every user by applying physiological measures of the subject. Also, physiological parameters obtained from experiment-based system identification may result in even more natural behavior and will supersede manual tuning. Third, the calculation of the reference trajectory could be improved. Customized mappings may account for varying predictors, i.e. individual gait patters. Also, different approaches to calculate reference trajectories may be tested [33].

Future experiments comparable to [15], [17], and [34] may reveal whether the bio-inspired control presented here can account for changes in speed and terrain in terms of adapting knee joint angle and moment.

In conclusion, it is noteworthy that the brain plasticity allows for long-term adaptation to the prosthesis. Also, short-term adaptations to changes in speed and the environment are possible [35]. To evolve an appropriate synergy between user and prosthesis, reflex-based user-cooperative controllers which take into account human adaptation are promising.

Acknowledgment

The authors would like to thank Stefania Bernasconi, Serge Pfeifer, Marco Bader and Michael Herold-Nadig for their valuable support with the development of the controller and the hardware, Selina Bühler, the team of BalgristTec and the Spinal Cord Injury Center for their help with the experiment and the subjects who participated.

References

[1] M. Grimmer and A. Seyfarth, "Mimicking human-like leg function in prosthetic limbs," in *Neuro-Robotics*. Springer, 2014, pp. 105–155.

[2] E. Perreault, L. Hargrove, D. Ludvig, H. Lee, and J. Sensinger, "Considering limb impedance in the design and control of prosthetic devices," in *Neuro-Robotics*. Springer, 2014, pp. 59–83.

[3] F. Sup, H. Varol, J. Mitchell, T. Withrow, and M. Goldfarb, "Self-contained powered knee and ankle prosthesis: Initial evaluation on a transfemoral amputee," in *Proc. IEEE 11th Int. Conf. Rehabil. Robot.*, 2009, pp. 638–644.

[4] J. Geeroms, L. Flynn, R. Jimenez-Fabian, B. Vanderborght, and D. Lefeber, "Ankle-knee prosthesis with powered ankle and energy transfer for CYBERLEGs α-prototype," in *Proc. IEEE Int. Conf. Rehabil. Robot. (ICORR)*, Jun. 2013, pp. 1–6.

[5] E. J. Rouse, L. M. Mooney, E. C. Martinez-Villalpando, and H. M. Herr, "Clutchable series-elastic actuator: Design of a robotic knee prosthesis for minimum energy consumption," in *Proc. IEEE Int. Conf. Rehabil. Robot. (ICORR)*, Jun. 2013, pp. 1–6.

[6] R. D. Gregg and J. W. Sensinger, "Biomimetic virtual constraint control of a transfemoral powered prosthetic leg," in *Proc. IEEE Amer. Control Conf. (ACC)*, Jun. 2013, pp. 5702–5708.

[7] B. E. Lawson, J. Mitchell, D. Truex, A. Shultz, E. Ledoux, and M. Goldfarb, "A robotic leg prosthesis: Design, control, and implementation," *IEEE Robot. Autom. Mag.*, vol. 21, no. 4, pp. 70–81, Dec. 2014.

[8] R. E. Kearney and I. W. Hunter, "System identification of human joint dynamics," *Critical Rev. Biomed. Eng.*, vol. 18, pp. 55–87, Feb. 1990.

[9] N. Aghasadeghi, H. Zhao, L. J. Hargrove, A. D. Ames, E. J. Perreault, and T. Bretl, "Learning impedance controller parameters for lower-limb prostheses," in *Proc. IEEE/RSJ Int. Conf. Intell. Robots Syst. (IROS)*, Nov. 2013, pp. 4268–4274.

[10] S. Pfeifer, H. Vallery, M. Hardegger, R. Riener, and E. J. Perreault, "Model-based estimation of knee stiffness," *IEEE Trans. Biomed. Eng.*, vol. 59, no. 9, pp. 2604–2612, Sep. 2012.

[11] S. Pfeifer, A. Pagel, R. Riener, and H. Vallery, "Actuator with angle-dependent elasticity for biomimetic transfemoral prostheses," *IEEE/ASME Trans. Mechatronics*, vol. 20, no. 3, pp. 1384–1394, Jun. 2015.

[12] E. P. Zehr and R. B. Stein, "What functions do reflexes serve during human locomotion?" *Prog. Neurobiol.*, vol. 58, no. 2, pp. 185–205, 1999.

[13] J. B. Nielsen and T. Sinkjær, "Afferent feedback in the control of human gait," *J. Electromyogr. Kinesiol.*, vol. 12, no. 3, pp. 213–217, 2002.

[14] H. Geyer, A. Seyfarth, and R. Blickhan, "Positive force feedback in bouncing gaits?" *Proc. R. Soc. B, Biol. Sci.*, vol. 270, no. 1529, pp. 2173–2183, 2003.

[15] H. Geyer and H. Herr, "A muscle-reflex model that encodes principles of legged mechanics produces human walking dynamics and muscle activities," *IEEE Trans. Neural Syst. Rehabil. Eng.*, vol. 18, no. 3, pp. 263–273, Jun. 2010.

[16] R. Desai and H. Geyer, "Muscle-reflex control of robust swing leg placement," in *Proc. IEEE Int. Conf. Robot. Autom. (ICRA)*, May 2013, pp. 2169–2174.

[17] M. Eilenberg, H. Geyer, and H. Herr, "Control of a powered ankle–foot prosthesis based on a neuromuscular model," *IEEE Trans. Neural Syst. Rehabil. Eng.*, vol. 18, no. 2, pp. 164–173, Apr. 2010.

[18] G. Ganesh, A. Albu-Schaffer, M. Haruno, M. Kawato, and E. Burdet, "Biomimetic motor behavior for simultaneous adaptation of force, impedance and trajectory in interaction tasks," in *Proc. IEEE Int. Conf. Robot. Autom. (ICRA)*, May 2010, pp. 2705–2711.

[19] H. Vallery, R. Burgkart, C. Hartmann, J. Mitternacht, R. Riener, and M. Buss, "Complementary limb motion estimation for the control of active knee prostheses," *Biomed. Technik*, vol. 56, no. 1, pp. 45–51, Feb. 2011.

[20] H. van der Kooij, B. Koopman, and F. C. van der Helm, "Human motion control," pp. 211–220, 2008.

[21] E. De Vlugt, A. C. Schouten, and F. C. van der Helm, "Quantification of intrinsic and reflexive properties during multijoint arm posture," *J. Neurosci. Methods*, vol. 155, no. 2, pp. 328–349, 2006.

[22] R. B. Stein and R. E. Kearney, "Nonlinear behavior of muscle reflexes at the human ankle joint," *J. Neurophysiol.*, vol. 73, no. 1, pp. 65–72, 1995.

[23] T. A. Boonstra, A. C. Schouten, and H. van der Kooij, "Identification of the contribution of the ankle and hip joints to multi-segmental balance control," *J. Neuroeng. Rehabil.*, vol. 10, no. 1, p. 23, 2013.

[24] R. Lozano, *Adaptive Control*, vol. 51, A. Isidori, Ed. Berlin, Germany: Springer 1998.

[25] E. D. Engeberg, "Human model reference adaptive control of a prosthetic hand," *J. Intell. Robot. Syst.*, vol. 72, no. 1, pp. 41–56, 2013.

[26] D. A. Winter, *Biomechanics and Motor Control of Human Movement*. Hoboken, NJ, USA: Wiley, 2009.

[27] A. Mourad and G. Keltoum, "A new approach to model reference adaptive control for nonlinear systems using virtual linearization," *Int. J. Electr. Power Eng.*, vol. 2, no. 2, pp. 104–108, 2008.

[28] N. Hovakimyan and C. Cao, $\mathcal{L}_1$ *Adaptive Control Theory: Guaranteed Robustness With Fast Adaptation*, vol. 21. Philadelphia, PA, USA: SIAM, 2010.

[29] H. B. Skinner, R. L. Barrack, S. D. Cook, and R. J. Haddad, Jr., "Joint position sense in total knee arthroplasty," *J. Orthopaedic Res.*, vol. 1, no. 3, pp. 276–283, 1983.

[30] T. Seel, J. Raisch, and T. Schauer, "IMU-based joint angle measurement for gait analysis," *Sensors*, vol. 14, no. 4, pp. 6891–6909, Jan. 2014.

[31] J. M. Jasiewicz *et al.*, "Gait event detection using linear accelerometers or angular velocity transducers in able-bodied and spinal-cord injured individuals," *Gait Posture*, vol. 24, no. 4, pp. 502–509, 2006.

[32] Q. Nguyen and K. Sreenath, "L_1 adaptive control for bipedal robots with control Lyapunov function based quadratic programs," in *Proc. IEEE Amer. Control Conf. (ACC)*, Jul. 2015, pp. 862–867.

[33] B. Koopman, E. H. van Asseldonk, and H. van der Kooij, "Speed-dependent reference joint trajectory generation for robotic gait support," *J. Biomech.*, vol. 47, no. 6, pp. 1447–1458, 2014.

[34] H. M. Herr and A. M. Grabowski, "Bionic ankle–foot prosthesis normalizes walking gait for persons with leg amputation," *Proc. R. Soc. B, Biol. Sci.*, vol. 279, no. 1728, pp. 457–464, 2012.

[35] A. C. H. Geurts and T. W. Mulder, "Reorganisation of postural control following lower limb amputation: Theoretical considerations and implications for rehabilitation," *Physiotherapy Theory Pract., Int. J. Phys. Therapy*, vol. 8, no. 3, pp. 145–157, 1992.

Anna Pagel received the Dipl.-Ing. degree in mechanical engineering from the Karlsruhe Institute of Technology, Germany, and the Ph.D. degree from ETH Zurich, Switzerland. Her research focuses on sensory feedback, joint impedance identification, and user-cooperative control strategies for actuated knee exoprostheses.

Raffaele Ranzani received the M.Sc. degree in robotics, systems and control from ETH Zurich, Switzerland, where he is currently pursuing the Ph.D. degree with the Rehabilitation Engineering Laboratory. His research focuses on control strategies for actuated knee exoprostheses, haptics, and human–machine interfaces in robot-assisted rehabilitation.

Robert Riener received the Dipl.-Ing. degree in mechanical engineering and the Ph.D. degree from TU Munich, Germany. He is currently the Head of the Sensory-Motor Systems Laboratory, ETH Zurich, and a Professor of medicine with the University of Zurich, Switzerland. His current research interests involve rehabilitation robotics, human motion synthesis, virtual reality, and man–machine interaction.

Heike Vallery received the Dipl.-Ing. degree in mechanical engineering from RWTH Aachen University, Germany, in 2004, and the Ph.D. degree from from TU Munich, Germany, in 2009. She is currently an Associate Professor with the Delft University of Technology, The Netherlands. Her research interests include the areas of bipedal locomotion, compliant actuation, and rehabilitation robotics.